Aero-structural design of an high-aspect ratio wing

Pietro Catalano* , Gianluca Diodati† , Davide Lucariello‡ , Pier Luigi Vitagliano §
CIRA Italian Aerospace Research Center, Capua (CE), 81043, Italy

The aero-structural design of an high aspect ratio wing has been performed by CIRA in the framework of the HERWINGT project supported by the Clean Aviation Joint Undertaking and funded by the European Union. The aim is to design an innovative wing suitable for the future hybrid-electric regional aircraft, that will contribute to the overall target to reduce fuel consumption, CO_2 and other GHG emissions, by improving the aerodynamic efficiency and reducing the weight. The wing has been designed and analyzed by a RANS flow solver in cruise and climb conditions and different loads factors have been considered for the determination of the loads acting on the wing. The primary structural weight has been evaluated by a quasi-analytical multi-stations tool with a genetic algorithm optimization implemented. Then the obtained structure has been validated through a FEM analysis

Nomenclature

$CIRA$	Italian Aerospace Research Center
C_p	Pressure coefficient
GHG	Green-house Gases
HER	Hybrid Electric regional
$KTAS$	Knote true air-speed
MOO	Multi Objective Optimization
MS	Margin of safety
nm	Nautical miles
n_z	Load factor
$RANS$	Reynolds Averaged Navier Stokes
FEM	Finite Emelemts Method
Re	Free-stream Reynolds number
t	Thickness
α	Angle of attack
γ	Intermittency function
κ	Turbulent kinetic energy
ω	Specific dissipation rate

I. Introduction

Greater attention to environmental aspects (even with stringent regulations) and higher market demand are changing the scenario of air mobility in the short range, centred on 500 km and up to 1000 km. Air vehicles operating in this range and operational environment (including regional aircraft with a capacity of up to 100 seats) are considered the first application in the scheduled air transport system that will adopt hybrid-electric propulsion technologies and associated complementary solutions for reducing the environmental footprint, toward climate-neutral aviation. Air vehicles operating at smaller distances or on thinner routes will also benefit from electric propulsion solutions tested on regional aircraft test-beds, by sharing the development of power modules and making use of different approaches to air vehicle integration.

*Researcher, p.catalano@cira.it, Fluid Mechanics Unit.
†Researcher, g.diodati@cira.it, Space Qualification Laboratory
‡Researcher, d.lucariello@cira.it, Structure and Materials Department
§Researcher, p.vitagliano@cira.it, Fluid Mechanics Unit.

CIRA is involved in the new Clean Aviation program with important participation in several projects, all dedicated to technological development for reducing the environmental impact of new-generation aircraft. In particular, the HERWINGT project (Hybrid Electric Regional Wing Integration Novel Wing Technologies) is supported by the Clean Aviation Joint Undertaking and funded by the European Union. The aim is to design an innovative wing suitable for the future hybrid-electric regional aircraft (HER), that will contribute to the overall target to reduce fuel consumption, CO_2 and other GHG emissions, by improving the aerodynamic efficiency and reducing the weight. The HERWINGT project will validate, down select, mature and demonstrate the concept, the architecture, the design and the key technologies for addressing an innovative wing design of a Hybrid Electric regional aircraft with a maximum capacity of 100 seats and a range of 500 to 1000 nm.

The focus of this paper is on the aero-structural design of a cantilever high-aspect ratio wing performed in the framework of the HERWINGT project.

II. Numerical Method

The methodology adopted is schematically showed in the figure 1. The loads are evaluated as follows:

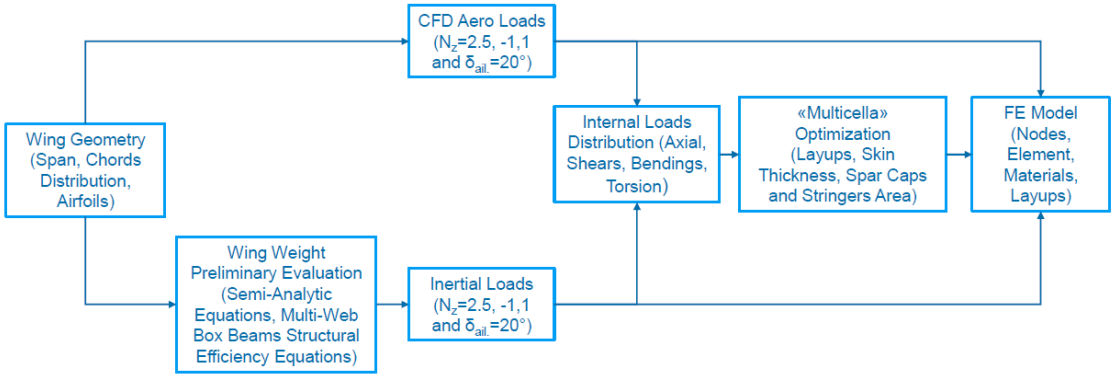

Fig. 1 Workflow of the aero-structural optimization of the high-aspect ratio cantilever wing

- the aerodynamic loads are evaluated with a CFD analysis. The in-house developed flow solver UZEN (Unsteady Zonal Euler Navier-Stokes) has been used. Three loads conditions are considered: Limit loads at cruise conditions with load factor $n_z = 2.5$, and -1, and deflection of 20° of the ailerons at $n_z = 1$;
- the inertial loads are evaluated in two distinct ways:
  - a simple quasi-analytical multi-station method based on multiweb box beam minimum weight analysis for the primary wing structure;
  - a semi-empirical method for the secondary wing structure.

The loads are then applied to the wing schematically idealized as a Euler beam, and the six internal loads characteristics (axial and shears forces, bendings and torsion moments) at several wing stations are calculated. These internal loads are then used as input for the "MULTICELLA" tool, a more refined quasi-analytical multi-stations tool with a genetic algorithm optimization implemented. After the optimization, a FE model was created from the output of the optimization process.

A. Aerodynamics

The numerical simulations for the assessment of the aerodynamic behaviour of the wing and for computing the aerodynamic loads have been performed by applying the CIRA in-house flow solver UZEN (**U**nsteady **Z**onal **E**uler **N**avier Stokes). This code solves the compressible RANS equations on structured multi-block domains. The adopted spatial discretization consists of a central finite-volume formulation with explicit blended 2^{nd} and 4^{th} order artificial dissipation. The dual-time stepping technique is employed for time-accurate simulations [1, 2]. The pseudo-time integration is carried out by an explicit hybrid multistage Runge-Kutta scheme. Classical convergence acceleration techniques, such as local time stepping and implicit residual smoothing, are available together with

multigrid algorithm. Turbulence is modelled by either algebraic or transport equation models [3, 4] and also hybrid RANS-LES methods are available [5]. UZEN is tipically used for simulating steady and unsteady flows around complex aeronautical configurations[6]. Some peculiar phenomena [2, 7] and particular devices [8, 9] can be reproduced.

The aerodynamic performances of the wing have been evaluated by applying the UZEN code adopting the SST $\kappa - \omega - \gamma$ [10] model. This model has been recently coded in UZEN and its implementation verified by test-cases of ERCOFTAC data-base, 2D airfoils and also a 3D 6 : 1 inclinate prolate spheroid [11, 12].

B. Internal Loads Distribution and Structural Arrangement Definition

The internal loads distributions are calculated by assuming the wing acting as a simple Euler beam with root fixed by the actual constraints. With these hypotheses, the axial force A_x, shear forces S_y and S_z, the torque moment T_y and the bending moments B_x and B_z are evaluated at a certain number of stations across the wing for the three cases considered. The aerodynamic and inertial loads are applied on the wing as follows:

- The aerodynamic load is a set of forces f_x, f_y and f_z applied on the wing surface mesh points;
- The inertial loads are the wing and fuel weight applied as spanwise linear distributions, and the propulsive system (engine plus nacelle) applied as a concentrated force.

The fuel and the engine weights are data problem. The mass of nacelle, ribs, secondary and primary wing structure are calculated as follows:

- A quasi-analytical Class II method for calculating the weights of the nacelle, the ribs and the secondary wing structure [13];
- A multi-station method based on a multiweb box beam minimum weight analysis based on efficiency equations for local and global buckling for the wing primary structure [14]..

Starting with a first trial for the total wing weight, a recursive method is adopted for the evaluation of this weight. At the end of the iterations, the internal loads distributions are then calculated.

With the multi-station method adopted, the optimum stringers and ribs spacing are also evaluated.

C. MULTICELLA Optimization Tool

An optimization tool named as "MULTICELLA" has been used. This tool is aimed at performing a preliminary sizing of a composite wing box structure, the sizing being based on composite strength and buckling. MULTICELLA is included in a Multi-Objective Genetic Algorithm optimization developed in MATLAB language.

MULTICELLA inputs are the wing-box geometry and structural arrangements (stringers and ribs spacing) and internal load distributions. MULTICELLA output is a Pareto front, constituted of design points of non-dominated optimal solutions: on the Pareto front, a solution that best fits the requirements of the design can be chosen (performing "a-postetiori" trade-off between non-dominated solutions). Figure 2 shows the block diagram of the MULTICELLA code operational flow. As optimization variables the thicknesses and areas of the different structural parts (wing box panels and stringers) of the wing box are chosen. Optimization objectives are the wing structural mass (to be minimized), and the strength and buckling Margin of Safety (MS) (to be maximized). The optimization phase is based on Genetic Algorithm due to its capabilities to explore a huge space constituted by a lot of design variables with numerous local maxima and minima.

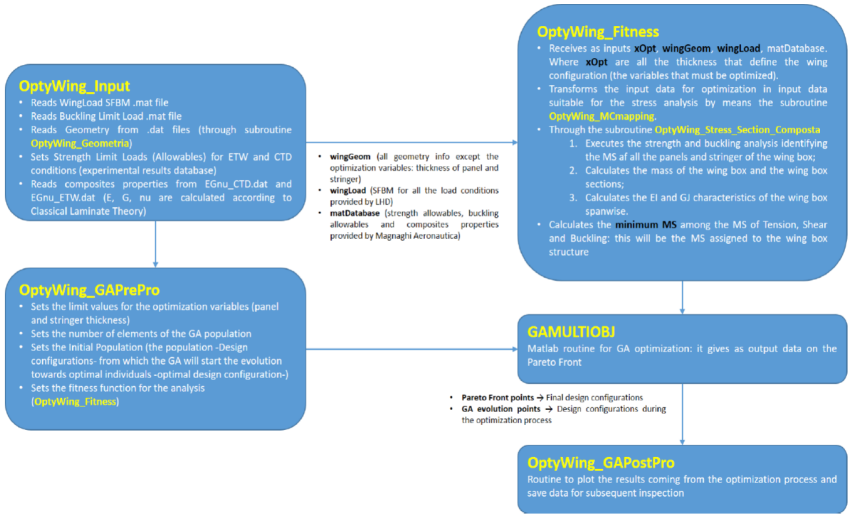

Fig. 2 Block diagram of MULTICELLA tool the high-aspect ratio cantilever wing

III. Results and Discussion

In the framework of the HERWINGT project, CIRA had the task to design a cantilever high-aspect ratio wing. The aim was to increase the efficiency by reducing the induced drag and keeping the structural weight limited. Both these goals have been achieved enlarging the span and the root chord with respect to a reference configuration with aspect ratio ≈ 12. Three wings with increasing span have been considered. Constraints were given on the tip chord and on

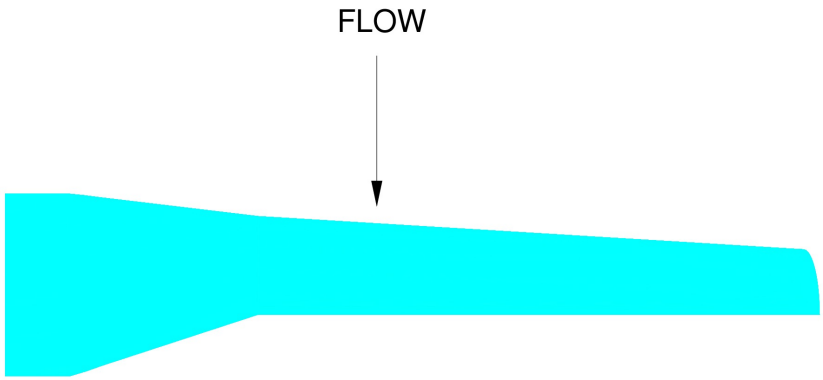

Fig. 3 Platform of the high-aspect ratio wing

the thickness of the wing sections. Also the position of the aerodynamic center and of the wing spars had to fulfill requirements for the integration with the fuselage.

The platform of the wings is shown in Figure 3. The main geometrical characteristics are:

- Surface: $72.75m^2$, $76.33m^2$, $79.83m^2$
- Span: $31.72m.$, $33.76m.$, $35.66m.$
- Aspect ratio: 13.83, 14.93, 15.93
- Root chord: $3.98m.$
- Kink chord: $2.15m.$
- Tip chord: $1.42m.$

The wings have been built using three different NACA 6-digits airfoils. The root airfoil has 19% relative thickness t/c,

the kink airfoil has 18%t/c and the tip airfoil 13.7%t/c. A linear lofting has been adopted to blend the wing surface. Wing twist distribution has been obtained after an optimisation Eulerian method aimed to minimize the induced drag in cruise conditions.

A. Aerodynamics

An aerodynamic trade-off analysis has been performed between the three wings named as Wing31, Wing33, and Wing35. A multi-block grid with 49 blocks and about 4.9×10^6 cells has been generated for all the grids. The topology

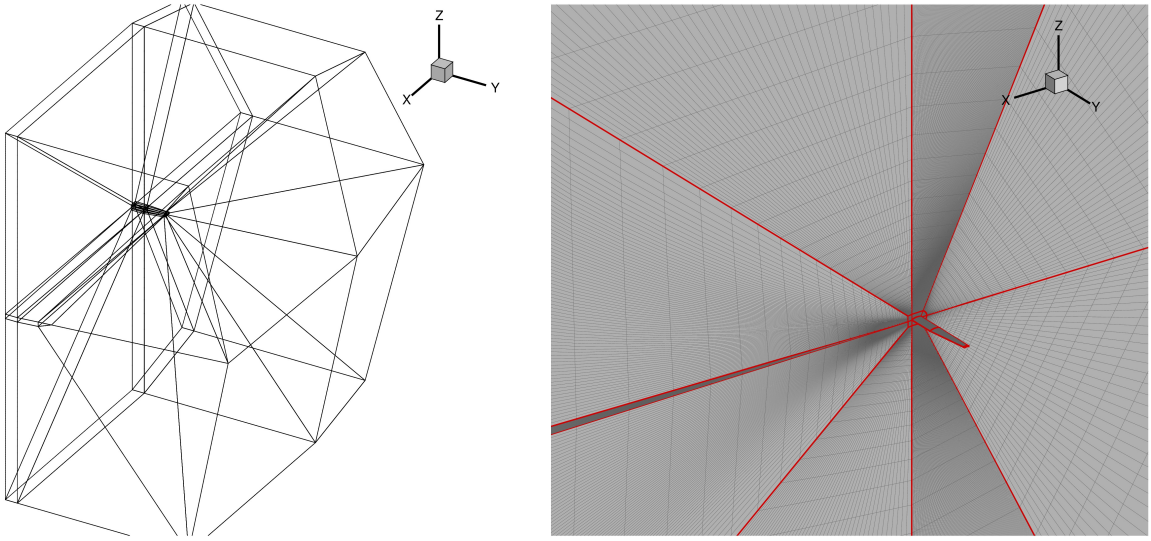

(a) Grid topology (b) Symmetry plane and wing

Fig. 4 Computational aerodynamic grid

and the mesh over the wing and in the symmetry plane are shown in figure 4.

RANS simulations by the in-house developed code UZEN employing the SST $\kappa - \omega - \gamma$ turbulence model [10] have been performed to simulate the flow around the wings. The aerodynamic performances are compared to a reference wing with a span of 29.4 m. and an aspect ratio of 12.

1. Cruise conditions

The cruise conditions are defined as an altitude of 25000 ft. at a speed of 300 KTAS. This means a Mach number of 0.50 and a Reynolds number per unit length of 5.51×10^6 1/m. The lift curve and the drag polar of the three novel wings are presented in figure 5. A comparison with the reference wing of aspect-ratio 12 is made. The highest C_L are obtained by the Wing35. A decrease in α_{ZL} is observed for the novel wings while the slope of the lift curve changes according to the wing span. It is worth noting that the ΔC_D is essentially due to the increase of aspect ratio. All the aerodynamic coefficients are evaluated by considering the same reference surface.

2. Climb conditions

The climb conditions consist in an altitude of 15000 ft. at a speed of 170 KCAS resulting in a Mach number of 0.34 and a Reynolds number per unit length of 5.14×10^6 1/m. The aerodynamic coefficients are reported in Figure 6. The results achieved for the Wing33 and Wing35 configurations are compared to the ones of the reference wing. The novel wings ensure a greater lift and a smaller drag with respect to the baseline configuration. Only the wings with 33 and 35 meters span have been analyzed because ensure a better efficiency than Wing31.

From the aerodynamic and structural results, it has turned out that the C_D decreases and the structural weight increases almost in a linear way with the wing span (figure 7). Eventually, the Wing35 has been selected for a deeper

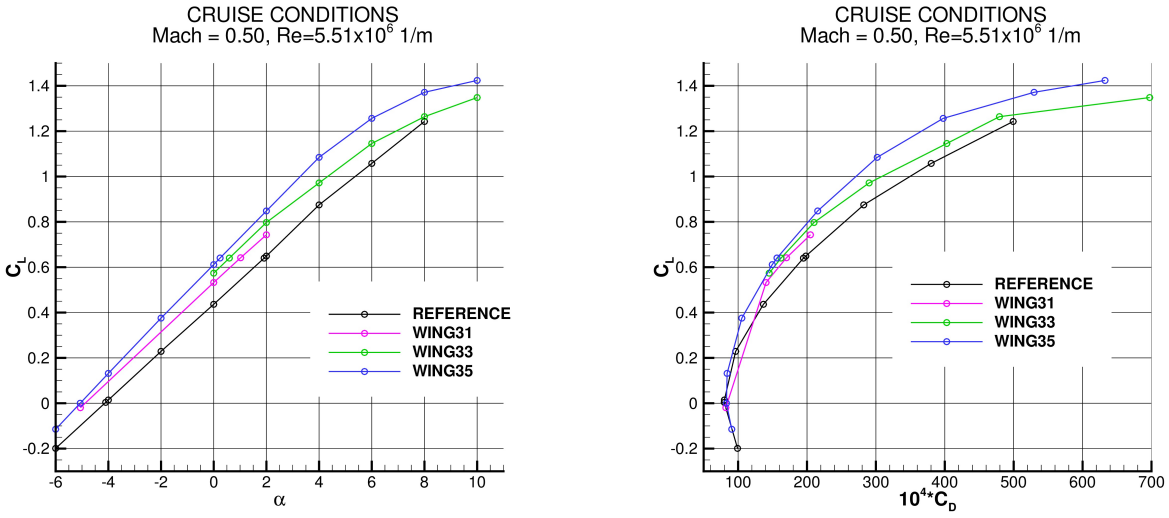

(a) Lift coefficient

(b) Drag Polar

Fig. 5 Aerodynamic coefficients in cruise conditions

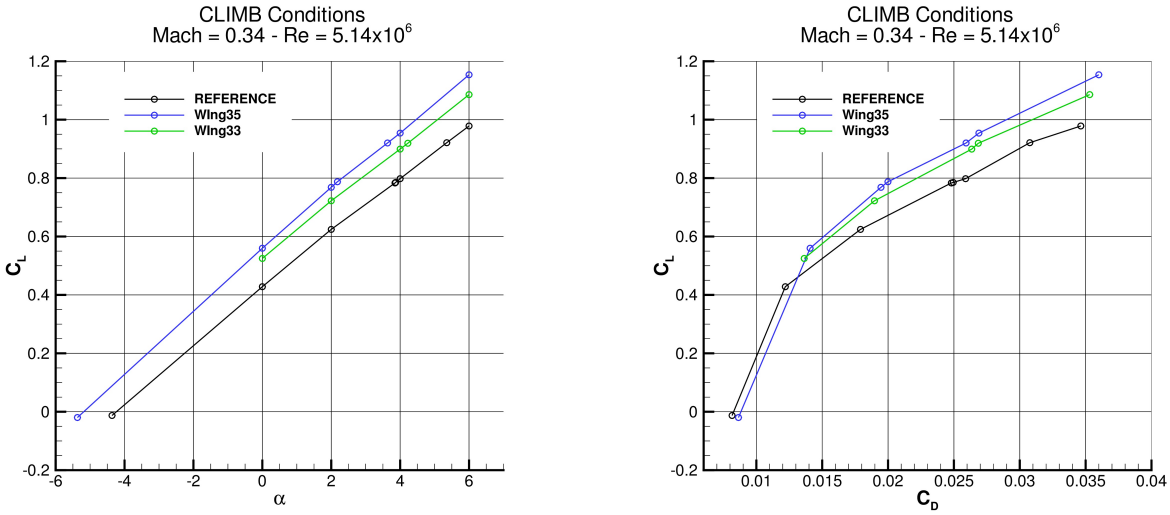

(a) Lift coefficient

(b) Drag Polar

Fig. 6 Aerodynamic coefficients in climb conditions

aero-structural analysis because the increment of the weight could be partly balanced with the decrease in C_D and in fuel consumption.

The drag polar at cruise conditions of Wing35 is reported in Figure 8. The induced part of the drag coefficient has been evaluated by subtracting the value of the drag coefficient at zero lift (C_{D0}) to the C_D. The agreement between the computed and theoretical induced drag results to be very good. This means that both the wings have an almost elliptic aerodynamic load distribution with an Oswald factor ≈ 1. Some little discrepancies can be noted only at the highest incidences where some flow separation occurs on the wing and prevents from obtaining a good comparison with the Prandtl curve.

The drag polar at climb conditions is shown in Figure 9. Again, the induced part of the C_D is evaluated and compared to the theoretical values. The agreement is not as good as for cruise conditions resulting in an Oswald factor of about 0.9.

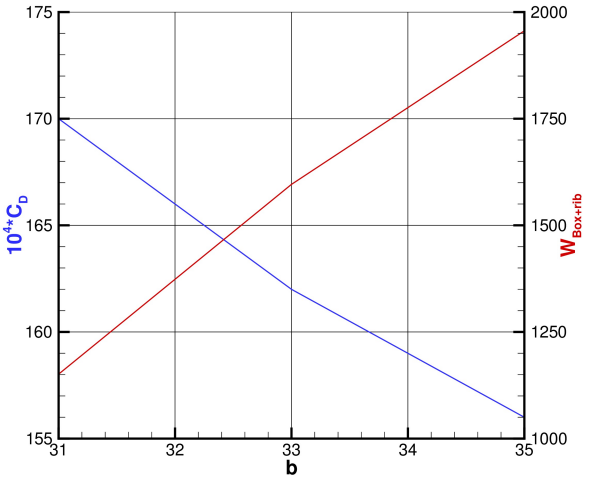

Fig. 7 Drag Coefficient and structural weight

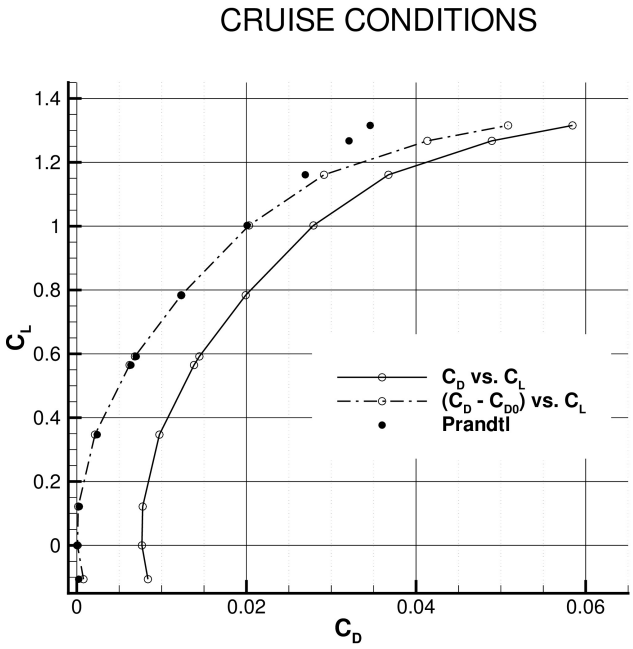

Fig. 8 Drag polar of Wing35 in cruise condition

The efficiency of the designed high aspect-ratio wing, is compared to the reference wing in Figure 10. The achieved gain at the design points is 8.2 (C_L=0.64) in cruise and 5.6 (C_L=0.92) in climb.

B. Aerodynamic Loads

Three loads distributions have been considered in order to evaluate the structural weight:

1) Cruise conditions with load factor $n_z = 2.5$
2) Cruise condition with load factor $n_{z=-1}$
3) Cruise condition with $n_z = 1$ and 20° deflection of the ailerons. As the true shape of the ailerons was not defined, a simple deformation of the rear part of the wing was produced, by rotating of 20 degrees the surface from 70%

Fig. 9 Drag polar of Wing35 in climb condition

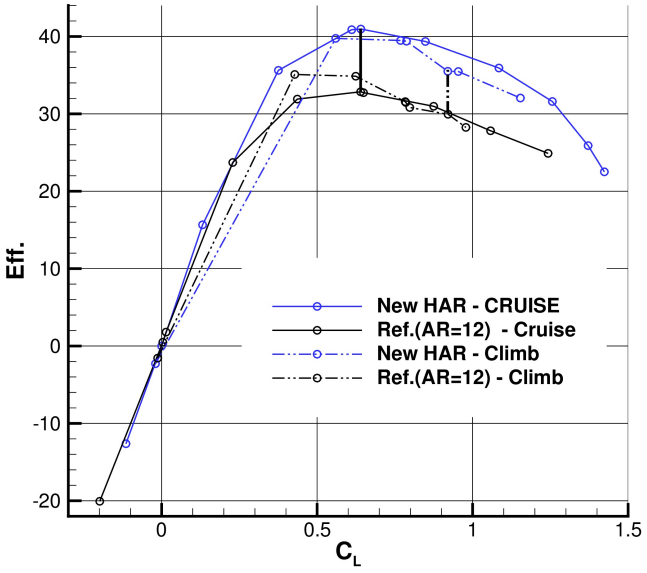

Fig. 10 Efficiency of the designed high aspect-ratio wing in cruise and climb condition

to 95% of the wing span starting from 73% of the local chord to the trailing edge.

Flow variables like pressure and viscous stress are computed at the cell centres of the CFD mesh. They are distributed to the mesh nodes on the wing surface by averaging the values of the cells surrounding each node for being used for the internal loads' definition. Dimensional concentrated forces are computed at each mesh point on the wing surface by summing the non-dimensional pressure and stress forces at each mesh node and multiplying the resulting force by the

free-stream dimensional pressure. A final correction factor is applied to all forces in order to guarantee that the total resulting force be equal to the required lift.

The set of aerodynamic loads for the structural analysis are provided as elementary forces applied on the nodes of the wing surface and integrated for obtaining the total forces. The internal loads distributions are then evaluated at the rib stations.

C. Structural Analysis

The CAD geometry of the wing is reported in figure 11. A three-spar wing-box is chosen for the large root chord

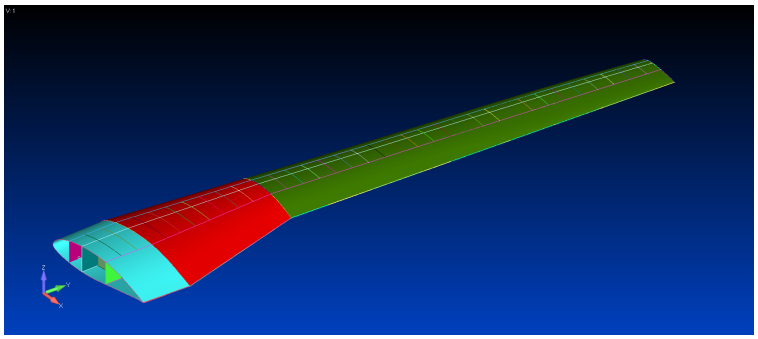

Fig. 11 CAD of the wing

adopted to avoid instability issues. For the ribs, a pitch of 500 mm was chosen, for 36 ribs in total; for the stringers, the maximum pitch at the root is about 200 mm, for 20 stringers in total. The number of stringers is kept constant along the wing span. For feasibility considerations, the wing is subdivided in 5 zone. In each zone the upper skin, the lower skin and the spar webs have each a constant thickness.

The internal loads of the wing are the inputs for an optimization process performed by the MULTICELLA tool. The structure should have adequate strength at a design condition. The primary purpose of the optimization process is to determine the structure which has a minimum weight, sufficient strength (MS at least equal to 0 everywhere) for all the assigned load conditions. The last step of the process is to identify the best solution among the various structural configurations obtained on the Pareto front coming out from MOO: the one that maximizes the MS and minimizes the overall weight of the wing.

Pareto front is a set of points that verifies the property that each one of these points is not dominated by another one (no point exists that has better properties on all the optimization objectives). On the Pareto fronts reported in Figure 12,

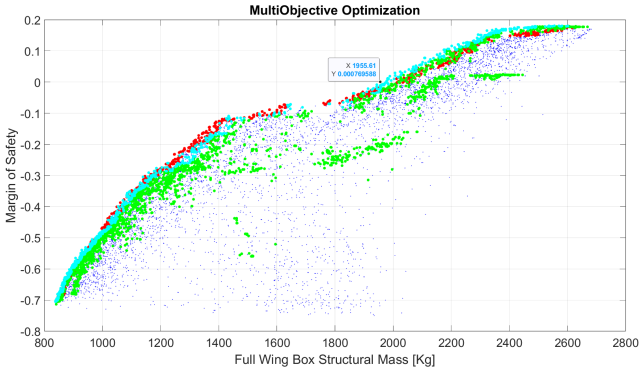

Fig. 12 Wing box optimization results

the blue points represent all the points analysed by the optimization algorithm for composite layups, with continuous thickness variability. The red points are definitely the Pareto points of the blue points. The green points are derived from

the red points and represent feasible optimization solutions (solutions compliant with layups with discrete thicknesses). The cyan points are a subset of the green points (best among them). The full wing box structural mass (without rib) is reported on the x-axis and the Margin of Safety of the structure (the minimum margin of safety -at strength and buckling- on the wing box) for all load conditions is reported on the y-axis.

1. Finite Elements Analysis

A FE model (figure 13) of the wing has been designed with the following characteristics:

- Nodes 10429
- Elements:
  - CQUAD4: 10500
  - RBE2: 37
  - RBE3: 7
  - CONM2: 43
  - CBAR: 3500
- Layups: 25
- MAT1: 100 (for CBAR elements)
- MAT8: 1 (for CQUAD elements)
- Properties: 168

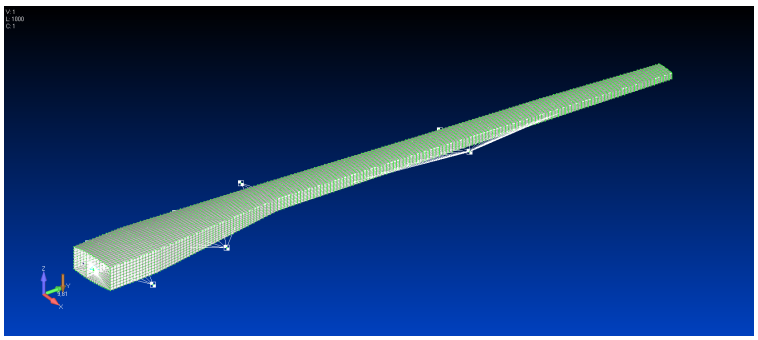

Fig. 13 FE model of the wing

The Margin of safety of the CBAR elements is greater than zero both for tensile and compressive cases. The laminate failure indices are shown in figure 14 and results greater than 1 in a very small portion of the wing. The zone in which

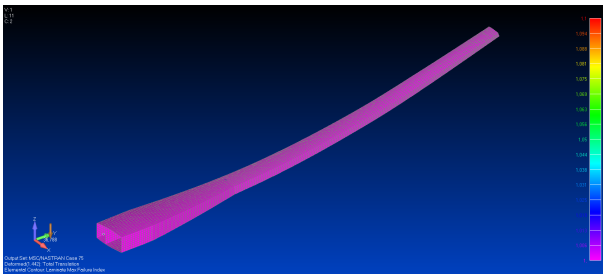

(a) CQUAD Laminate failure index

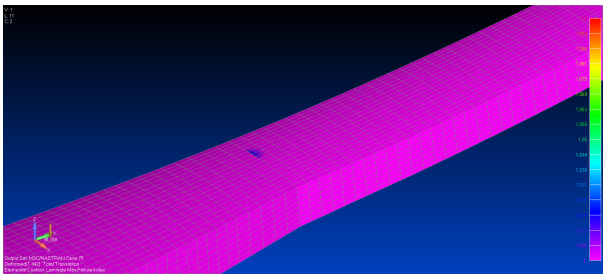

(b) CQUAD Laminate failure index - zoom

Fig. 14 CQUAD Laminate failure index

the failure index is very slightly greater than 1 is where the RBE3 element simulate the wing-engine attachment. Due to this reason and the small extension of the zone, no modifications are introduced in the model to reduce this failure index.

Buckling analyses have been performed for all the three load conditions considered. The buckling eigenvalues are 1.02, 1.05, and 1.21 for the load conditions 1, 2, and 3 respectively meaning that the load to obtain the instability

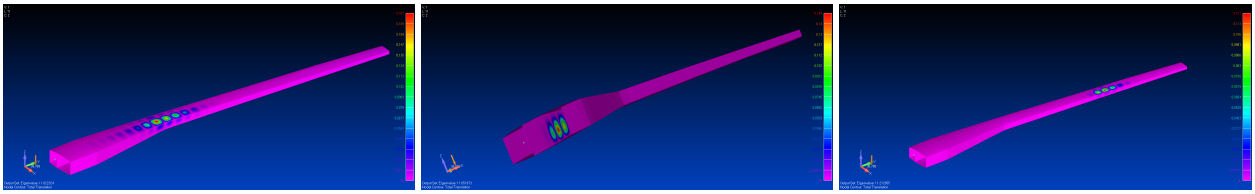

(a) Load condition 1 (b) Load condition 2 (c) Load condition 3

Fig. 15 Buckling conditions

depicted in the zone of the wing shown in figure 15 should be 2%, 5%, and 21% greater than the applied one.

All the analyses performed have shown that the wing is able to sustain the ultimate loads introduced.

IV. Conclusions

Activities performed for the aero-structural design of a high-aspect ratio cantilever wing have been presented and discussed. This asset is part of the HERWINGT (Hybrid Electric Regional Wing Integration Novel Wing Technologies) project supported by the Clean Aviation Joint Undertaking and funded by the European Union.

First, starting from a baseline configuration, three novels wings with increasing span and aspect ratio has been proposed and evaluated following the specifications and requirements delivered in the framework of the HERWINGT project. The aerodynamic design has been driven by the requirement of reducing both induced drag and structural weight. Both the goals have been achieved with a span and root chord larger than the baseline wing. It has been verified as the decrease of the drag coefficient is essentially induced drag that fits very well with the Prandtl theory. The wings have been analysed by a CFD method and numerical simulations performed in cruise and climb conditions by an in-house developed RANS flow solver. Cruise and climb conditions have been considered. It has turned out that the C_D and the structural weight linearly decrease and increase with the span respectively. The Oswald factor has resulted to be 1 in cruise and 0.9 in climb.

Then, an aero-structural procedure has been applied for one selected wing. The aerodynamic loads have been computed in cruise conditions with a load factor 2.5 and -1 and load factor 1 with a deflection of the ailerons of 20°. The loads are used, after a post-processing phase, for a structural analysis aimed at the evaluation of the weight of the wing box. The inertial loads are evaluated by a simple quasi-analytical multi-station method for the primary wing structure and a semi-empirical method for the secondary wing structure. The loads are applied to the wing schematically idealized as an Euler beam, and used as input for the in-house developed weight optimization tool. The finite elements model of the wing has been finally generated from the output of the optimization process.

The final chosen wing has a span of 35 m. with an aspect ratio of 15.93 with again in the efficiency of about 25% in cruise and 19% in climb with a primary structural weight about 25% greater than the baseline wing.

V. Ackowledgements

This study is part of the Hybrid Electric Regional Wing Integration Novel Green Technologies project (HERWINGT). This project has received funding from the Clean Aviation Joint Undertaking under the European Union's Horizon Europe research and innovation programme under grant agreement ID 101102010 (https://doi.org/10.3030/101102010). Views and opinions expressed are however those of the author(s) only and do not necessarily reflect those of the European Union or the Clean Aviation Joint Undertaking. Neither the European Union nor the granting authority can be held responsible for them.

References

[1] Marongiu, C., Catalano, P., Amato, M., and Iaccarino, G., "U-ZEN : A computational tool solving U-RANS equations for industrial unsteady applications," 34^{th} *AIAA Fluid Dynamics Conference*, 2004. AIAA Paper 2004-2345.

[2] Capizzano, F., Catalano, P., Marongiu, C., and Vitagliano, P. L., "U-RANS Modelling of Turbulent Flows Controlled by Synthetic Jets," 35^{th} *AIAA Fluid Dynamcis Conference*, 2005. AIAA paper 2005-5015.

[3] Catalano, P., and Tognaccini, R., "Turbulence modelling for low Reynolds number flows," *AIAA Journal*, Vol. 48, 2010, pp. 1673–1685.

[4] Catalano, P., Mele, B., and Tognaccini, R., "On the implementation of a turbulence model for low Reynolds number flows," *Computers and Fluids*, Vol. 109, 2015, pp. 67–71.

[5] Catalano, P., "Application of a Hybrid RANS-LES method to free shear layers flows." *ASME International Mechanical Engineering Congress & Exposition, IMECE 2019*, 2019. IMECE 2019-10618.

[6] Eliasson, P., Catalano, P., Pape, M.-C., Ortmann, J., Pelizzari, E., and Ponsin, J., "Improved CFD predictions for high lift flows in the European project EUROLIFT II," *AIAA Paper 2007-4303*, 2007.

[7] Iaccarino, G., Marongiu, C., Catalano, P., and Amato, M., "RANS Modeling and Simulation of Synthetic Jets," *AIAA paper 2004-2223*, 2004.

[8] Catalano, P., De Rosa, D., Mele, B., Tognaccini, R., and Moens, F., "Performance improvements of a regional aircraft by riblets and natural laminar flow," *Journal of Aircraft*, Vol. 57, No. 1, 2020, pp. 29–40.

[9] Marino, A., Catalano, P., Marongiu, C., Peschke, P., Hollenstein, C., and Donelli, R., "Effect of high voltage pulsed DBD plasma on the aerodynamic performances in subsonic and transonic conditions," 43^{rd} *AIAA Fluid Dynamics Conference*, 2013. AIAA paper 2013-2752.

[10] Menter, F. R., Smirnov, P. E., Liu, T., and Avancha, R., "A One-Equation Local Correlation-Based Transition Model," *Flow, Turbulence and Combustion*, Vol. 95, No. 4, 2015, pp. 583–619. doi:10.1007/s10494-015-9622-4, URL `http://dx.doi.org/10.1007/s10494-015-9622-4`.

[11] De Rosa, D., and Catalano, P., "Validation of intermittency model for transition prediction in a RANS flow solver," *AIAA Aerospace Sciences Meeting, 2018*, , No. 210059, 2018.

[12] de Rosa, D., and Catalano, P., "RANS simulations of transitional flow by γ model," *International Journal of Computational Fluid Dynamics*, 2019.

[13] Torenbeek, E., *Advanced Aircraft Design – Conceptual Design, Analysis and Optimization of Subsonic Civil Aircraft*, Wiley, 2013.

[14] Ardema, M., Chambers, M., Patron, A. P., Hahn, A. S., Miura, M., and Moore, M. D., "Analytical Fuselage and Wing Weight Estimation of Transport Aircraft," Tech. Rep. NASA-TM-110392, NASA, 1996.